Quantitative Techniques for Assessing and Controlling the Dispersion and Biological Effects of Multiwalled Carbon Nanotubes in Mammalian Tissue Culture Cells

Xiang Wang,[†,‡,¶] Tian Xia,[†,‡,¶] Susana Addo Ntim,[§] Zhaoxia Ji,[‡] Saji George,[†,‡] Huan Meng,[†,‡] Haiyuan Zhang,[†,‡] Vincent Castranova,[⊥] Somenath Mitra,[§] and André E. Nel[†,‡,*]

[†]Division of NanoMedicine, Department of Medicine, University of California, Los Angeles, California 90095, United States, [‡]California NanoSystems Institute, University of California, Los Angeles, California 90095, United States, [§]Department of Chemistry and Environmental Science, New Jersey Institute of Technology, Newark, New Jersey 07102, United States, and [⊥]NIOSH, 1095 Willowdale Road, Morgantown, West Virginia 26505, United States. [¶]These authors contributed equally to this work.

ABSTRACT *In vivo* studies have demonstrated that the state of dispersion of carbon nanotubes (CNTs) plays an important role in generating adverse pulmonary effects. However, little has been done to develop reproducible and quantifiable dispersion techniques to conduct mechanistic studies *in vitro*. This study was to evaluate the dispersion of multiwalled carbon nanotubes (MWCNTs) in tissue culture media, with particular emphasis on understanding the forces that govern agglomeration and how to modify these forces. Quantitative techniques such as hydrophobicity index, suspension stability index, attachment efficiency, and dynamic light scattering were used to assess the effects of agglomeration and dispersion of as-prepared (AP), purified (PD), or carboxylated (COOH) MWCNTs on bronchial epithelial and fibroblast cell lines. We found that hydrophobicity is the major factor determining AP- and PD-MWCNT agglomeration in tissue culture media but that the ionic strength is the main factor determining COOH-MWCNT suspendability. Bovine serum albumin (BSA) was an effective dispersant for MWCNTs, providing steric and electrosteric hindrances that are capable of overcoming hydrophobic attachment and the electrostatic screening of double layer formation in ionic media. Thus, BSA was capable of stabilizing all tube versions. Dipalmitoylphosphatidylcholine (DPPC) provided additional stability for AP-MWCNTs in epithelial growth medium (BEGM). While the dispersion state did not affect cytotoxicity, improved dispersion of AP- and PD-MWCNTs increased TGF-β1 production in epithelial cells and fibroblast proliferation. In summary, we demonstrate how quantitative techniques can be used to assess the agglomeration state of MWCNTs when conducting mechanistic studies on the effects of dispersion on tissue culture cells.

KEYWORDS: multiwalled carbon nanotubes (MWCNTs) · dispersion · hydrophobicity · ionic strength · bovine serum albumin · steric hindrance · cell culture medium

Carbon nanotubes (CNTs) were first described in 1991.[1] This type of carbon allotrope exhibits a high surface area, high mechanical strength, ultralight weight, enhanced electrical conductivity, and excellent chemical as well as thermal stability.[2] Because of these novel properties CNTs are being used for a wide range of applications such as electronics, field emission devices, energy storage devices, sensors and drug delivery devices.[3,4] However, in spite of their obvious commercial value, the safety of these materials needs to be considered in occupational, consumer, and environmental settings. At least two important toxicological scenarios have emerged that raise safety concerns, namely the ability of multiwalled and single-walled CNTs to generate granulomatous inflammation or fibrotic responses in the lung as well as mesothelial inflammation in rodents.[5−10] While similar pathology or disease processes have not been described for multiwalled carbon nanotubes (MWCNTs) in humans, the animal studies point to the importance of establishing screening procedures to assess CNT safety as well as avoidance of inhalation exposures in the workplace.[11]

To plan and conduct reproducible biological experiments, it is important to evaluate the physicochemical characteristics that influence CNT bioavailability and interactions at the nanobio interface. One of the key physicochemical characteristics that determine biological responses in the rodent lung is the state of CNT dispersion, with agglomerated CNTs more prone to be deposited in the proximal airway where they induce granulomatous inflammation as compared to better dispersed tubes that are capable of deposition in alveoli and interstitial spaces, where they elicit interstitial fibrosis.[12] It is important, therefore, to understand the effects of the biological media on the characteristics of CNTs, particularly their state of suspension and how that influences bioavailability and biological outcome. It is also important to understand how to control the state of CNT agglomeration under biological conditions to compare the clumped with the better dispersed

*Address correspondence to anel@mednet.ucla.edu.

Received for review August 23, 2010 and accepted October 31, 2010.

Published online November 10, 2010.
10.1021/nn102112b

© 2010 American Chemical Society

tubes. Some of the key factors involved in CNT agglomeration are hydrophobicity, attractive van der Waals forces, and the potential influence of electrical double layer formation on the surface of functionalized CNTs.[13] While it is known that CNTs can be transiently deagglomerated by mechanical methods such as vortexing and sonication, appropriate dispersants are needed to stabilize the tube suspensions through provision of steric hindrance, electrostatic or electrosteric effects. Although effective dispersants such as *N*,*N*-dimethylformamide (DMF), *N*-methylpyrrolidone (NMP),[14,15] or natural organic matter (NOM)[16−18] have been identified, these are not appropriate for studying CNT effects under tissue culture conditions. However, a number of proteins and nontoxic surfactants have emerged that could be applied to control the state of tube dispersion in biological conditions. For example, fetal bovine serum (FBS) is a useful dispersant in tissue culture media,[19,20] while *in vivo* studies have identified the effectiveness of 1% Tween 80 as a dispersant in phosphate-buffered saline (PBS).[6,8] In addition, Dr. Castranova and colleagues have reported the use of lung lining fluid obtained by bronchoalveolar lavage (BAL) of rodents as an effective dispersing medium for carbon-based nanoparticles.[21] The same group also formulated an artificial lung lining fluid that can be reconstituted through the mixing of serum albumin with the phospholipid surfactant, dipalmitoylphosphatidylcholine (DPPC).[22] Indeed, independent studies have confirmed the synergistic effects of proteins and surfactants in CNT dispersion.[23,24] Finally, it is important to point out that most of the aforementioned studies have been executed on single or a limited number of tube formulations that did not include a systematic variation in CNT physicochemical properties to compare dispersants that are specifically chosen to modify tube behavior in buffered ionic conditions.

In this study, we used purified (PD) and carboxyl-functionalized (COOH) derivatives of as-prepared (AP) MWCNTs to develop quantitative methods for assessing the suspension of these tubes in water and tissue culture media, including the use of these methods to select for the optimal dispersion to perform mechanistic cell culture studies. We demonstrate the practical use of a partitioning coefficient, suspension stability index, attachment efficiency, and dynamic light scattering (DLS) in a systematic approach to stabilization of MWCNT suspension through the use of BSA and DPPC. We demonstrate that BSA and DPPC function in additive fashion to disperse hydrophobic AP-MWCNTs in an epithelial growth medium and that this leads to increased TGF-β1 production in a bronchial epithelial cell line. Moreover, better-dispersed MWCNTs also increased fibroblast proliferation, in agreement with similar observations in the rodent lung.[7,12] Quantifiable methods to determine the state of CNT dispersal will be of great benefit in executing biological experiments on these materials.

TABLE 1. Physicochemical Characterization of the MWCNTs[a]

	AP-MWCNT	PD-MWCNT	COOH-MWCNT
outer diameter (nm)	20−30	20−30	20−30
inner diameter (nm)	5−10	5−10	5−10
length (μm)	10−30	10−30	10−30
purity	around 94%	>95%	>95%
impurities (wt %)	4.49% Ni, 0.76% Fe	1.80% Ni, 0.08% Fe	0.18% S

[a]The outer and inner diameter and length distribution were measured using the SEM images of the MWCNTs. The purity was measured by thermogravimetric analyses (TGA) using a Pyris 1 TGA (Perkin-Elmer Inc., Covina, CA). The elemental composition was analyzed by energy dispersive X-ray spectroscopy (EDS, Oxford Instrument, Oxfordshire, UK). The experiment details are described in the Materials and Methods.

RESULTS AND DISCUSSION

Characterization of MWCNT. The original supply of AP-MWCNTs from Cheap Tubes, Inc. served as the stock for preparing purified (PD) and carboxylated (COOH) derivatives. This derivatization provided a small library of materials that could be systematically compared for the influence of hydrophobicity, hydrophilicity, and electrical double layer formation on tube agglomeration in biological media and the resultant effect on the cell biological responses. The baseline physicochemical characteristics of the materials are listed in Table 1. While AP-MWCNTs contained ~5.25 wt % metal impurities, purification decreased this to ~1.88 wt %. Further acid treatment of the PD-MWCNTs introduced carboxyl groups on 5.27% of the carbon backbone (on a per weight basis). The carboxyl functionalization considerably increased the negative surface charge on the tubes, which makes them more hydrophilic but at the same time lays the platform for electrical double layer formation that could affect COOH-MWCNT dispersion according to the tenets of Derjaguin, Landau, Verwey, and Overbeek (DLVO) theory.[25] The structure of the MWCNT was further analyzed by SEM and FTIR spectroscopy as demonstrated in Figure 1. The SEM images show that acid treatment did not cause structural damage, allowing the tubes to remain intact (Figure 1 A). FTIR spectroscopy confirmed the carboxyl functionalization (Figure 1 B).

Assessment of the Contribution of Hydrophobicity in AP- and PD-MWCNT Agglomeration and Preventing This Attachment by Steric and Electrosteric Hindrance. We used *n*-octanol/water partitioning to establish a hydrophobicity index for the different MWCNT derivatives (Figure 2). This index was calculated using the light absorbance of AP-MWCNT, PD-MWCNT, and COOH-MWCNT at 550 nm wavelength in water or other aqueous media prior to as well as following *n*-octanol introduction as demonstrated in Figure 2A. Figure 2B compares the relative hydrophobicity indices of the tubes in distilled H_2O, phenol red-free Dulbecco's Modified Eagle's Medium (DMEM) and Bron-

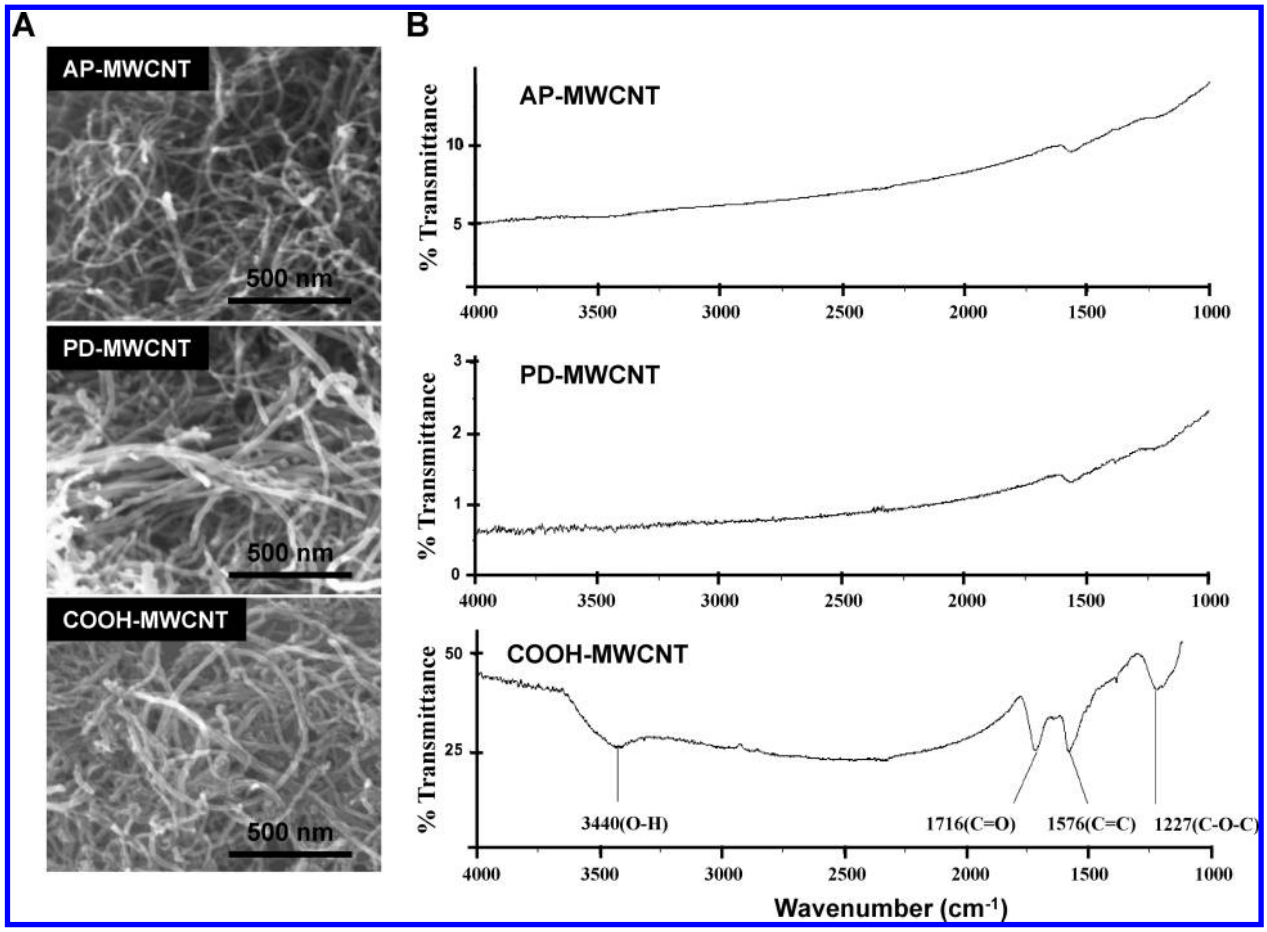

Figure 1. Physicochemical characterization of the AP-MWCNT, PD-MWCNT, and COOH-MWCNT. (A) Representative scanning electronic microscopy (SEM) images of AP-MWCNT, PD-MWCNT, and COOH-MWCNT. Pictures were taken with a Genesis 4000 XMS SEM, (EDAX Inc., Mahwah, NJ). Magnification is 200 000×. (B) The Fourier transform infrared spectroscopy spectra done by a PerkinElmer Spectrum One instrument (Downers Grove, IL) show the carboxyl functionalization of the COOH-MWCNT.

chial Epithelial Basal Medium (BEBM). DMEM is a widely used tissue culture medium while BEBM is used for culturing bronchial epithelial cells.[26,27] The results show that while AP- and PD-MWCNTs had relatively high hydrophobicity indices, favoring partitioning in the *n*-octanol phase, the COOH-MWCNTs were more hydrophilic and favored partitioning in the aqueous phase (Figure 2B). Visual inspection of the phases confirmed that while AP-MWCNTs and PD-MWCNTs were located in the *n*-octanol layer or close to the interface (arrows), COOH-MWCNTs were homogeneously dispersed in the water or tissue culture media (Supporting Information, Figure S1, upper panel). The hydrophilicity of the carboxylated tubes agrees with their relatively high negative surface charge (zeta-potential of −50.30 mV) in water (Table 2), which provides electrostatic repulsion. In contrast, AP-MWCNTs and PD-MWCNTs exhibited slightly negative zeta-potentials of −14.5 and −8.73

TABLE 2. Zeta Potential and Hydrodynamic Size of the MWCNTs[a]

		AP-MWCNT	PD-MWCNT	COOH-MWCNT
Zeta potential (mV)	in H_2O (with BSA)	−14.50 (−28.61)	−8.73 (−31.76)	−50.30 (−29.35)
	in PBS (with BSA)	−14.08 (−10.94)	−13.12 (−11.31)	−13.08 (−10.13)
	in BEGM (with BSA)	−8.01 (−11.80)	−7.42 (−11.80)	−9.12 (−11.80)
	in DMEM (with BSA)	−12.85 (−7.22)	−13.20 (−9.64)	−13.45 (−11.13)
Hydrodynamic size by DLS (nm)	in H_2O (with BSA)	324 (264)	858 (313)	134 (161)
	in PBS (with BSA)	713 (362)	718 (304)	1193 (243)
	in BEGM (with BSA)	779 (239)	650 (242)	1062 (310)
	in DMEM (with BSA)	1390 (248)	1492 (295)	1529 (230)

[a]The zeta potential measurement of the MWCNT suspension was performed using a ZetaSizer Nano-ZS instrument (Malvern Instruments, Worcestershire WR, UK). The MWCNTs were suspended by sonication as described in Materials and Methods in the absence or presence of 0.6 mg/mL BSA. The MWCNT hydrodynamic size in H_2O, PBS, BEGM, and DMEM were measured using the dynamic light scattering (HT-DLS, Dynapro Plate Reader, Wyatt Technology, Santa Barbara, CA). The experiment details are described in the Materials and Methods.

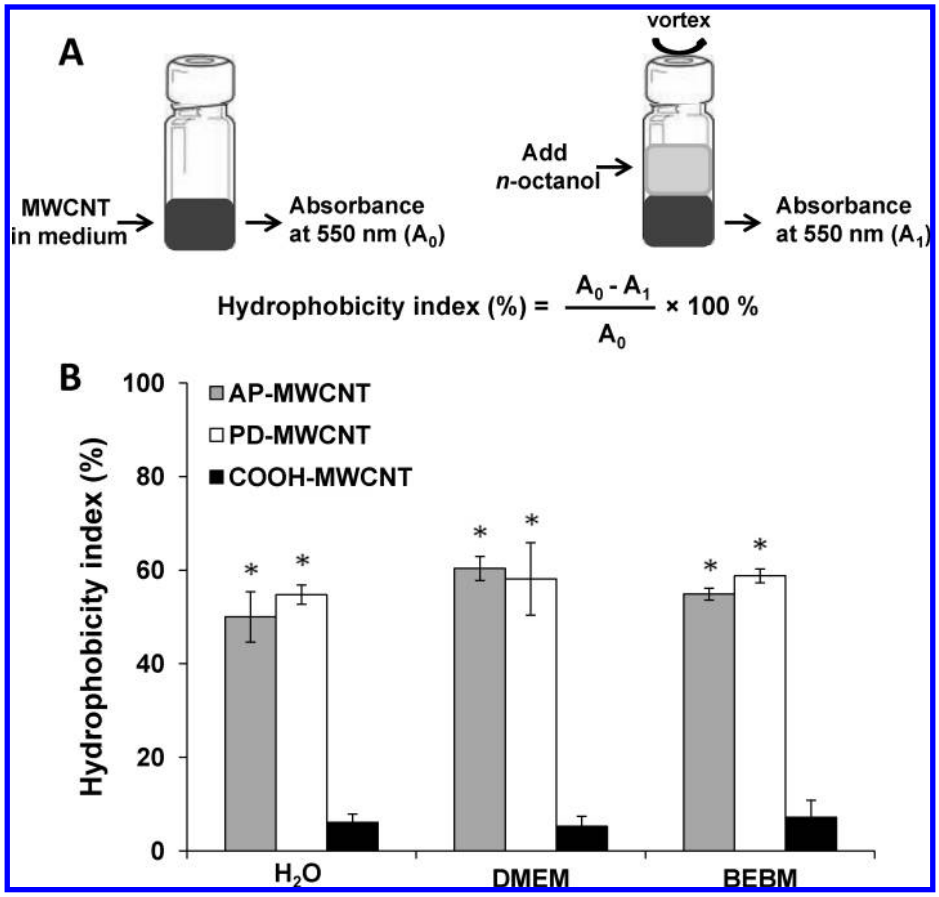

Figure 2. Determination of the hydrophobicity index of AP-, PD- and COOH-MWCNT in H_2O, DMEM, and BEBM using partitioning in an *n*-octanol/aqueous interface. The hydrophobicity index of the tubes suspended in the aqueous phase at 50 μg/mL was calculated by the absorbance reading at 550 nm in H_2O, DMEM, and BEBM (A_0) prior to and following (A_1) the addition of *n*-octanol as described in Materials and Methods. The same experiment was carried out at different CNT concentrations (up to 120 μg/mL), which yielded the same results, and therefore was incorporated into the biological experiments (*e.g.*, Figure 6) with the same trend. The asterisk (*) indicates $p < 0.05$, compared to the COOH-MWCNT.

mV, respectively. Please notice that although the experiment in Figure 2 was conducted at a MWCNT concentration of 50 μg/mL, similar trends were obtained with either lower (25 μg/mL) or higher (100 μg/mL) concentrations (not shown). All considered, the relatively high hydrophobicity of AP-MWCNTs and PD-MWCNTs is a major factor contributing to their attachment in aqueous environments, while the electrostatic repulsion by their carboxyl groups promotes COOH-MWCNT hydrophilicity.

To limit the extent of MWCNT agglomeration for performing pulmonary exposure studies, it has been demonstrated by simple visual inspection approaches that the dispersion of single-walled carbon nanotubes (SWCNTs) and MWCNTs can be improved by a surrogate lung lining fluid that is composed of serum albumin mixed with a surfactant, DPPC.[22] When BSA was introduced to the aqueous AP-MWCNT and PD-MWCNT suspensions during sonication, it could immediately be ascertained following *n*-octanol introduction that the tubes prefer the aqueous environment (water or tissue culture medium) in which they remain stably suspended (Supporting Information, Figure S1, lower panel). Interestingly, the addition of BSA changed the zeta-potentials of AP-MWCNTs and PD-MWCNTs from −14.50 to −28.61 mV and −8.73 to −31.76 mV (Table 2), respectively. This is due to direct BSA binding to the hydrophobic tube surfaces.[28] Once attached to the tube surfaces by sonication, flexible macromolecules such as BSA (hydrodynamic radius of ~7.5 nm by DLS) are capable of providing steric hindrance.[28] In addition, because of BSA's isoelectric point of ~4.7, this protein becomes anionic at pH ≥ 7, which explains the increased negative zeta-potential. This effect could contribute to electrosteric hindrance. Therefore, the major effect of BSA in stabilizing hydrophobic AP- and PD-MWCNTs in water is through steric hindrance as well as electrosteric repulsion. By contrast, the major BSA influence on the hydrophilic COOH-MWCNTs is a steric hindrance effect. While it is known that a number of proteins (e.g., serum albumin, immunoglobulin, streptavidin) are capable of nonspecific binding to CNT surfaces,[29] no previous effort has been made to quantify the degree of dispersal.

The Effect of Ionic Strength on Tube Agglomeration in Physiological Media. While ionic strength has no independent discernible effect on AP- and PD-MWCNT agglomeration (Supporting Information, Figure S2), the aqueous dispersion of COOH-MWCNT is clearly influenced by the addition of ionic charge, as demonstrated by the progressive decline of the suspension stability index with incremental concentrations of PBS (Figure 3A). The addition of 0.9% saline (Figure 3C) or salt-containing biological media (Supporting Information, Figure S3) had similar destabilizing effects. According to the DLVO theory, the stability of a colloidal suspension is based on the net balance of two predominant forces, namely electrostatic repulsion that prevents and attractive van der Waals forces that promote agglomeration.[25] While in distilled water or dilute electrolyte solutions, the high negative wall surface potential of COOH-MWCNTs is capable of overwhelming the van der Waals attractions, the addition of ionic charge leads to double layer for-

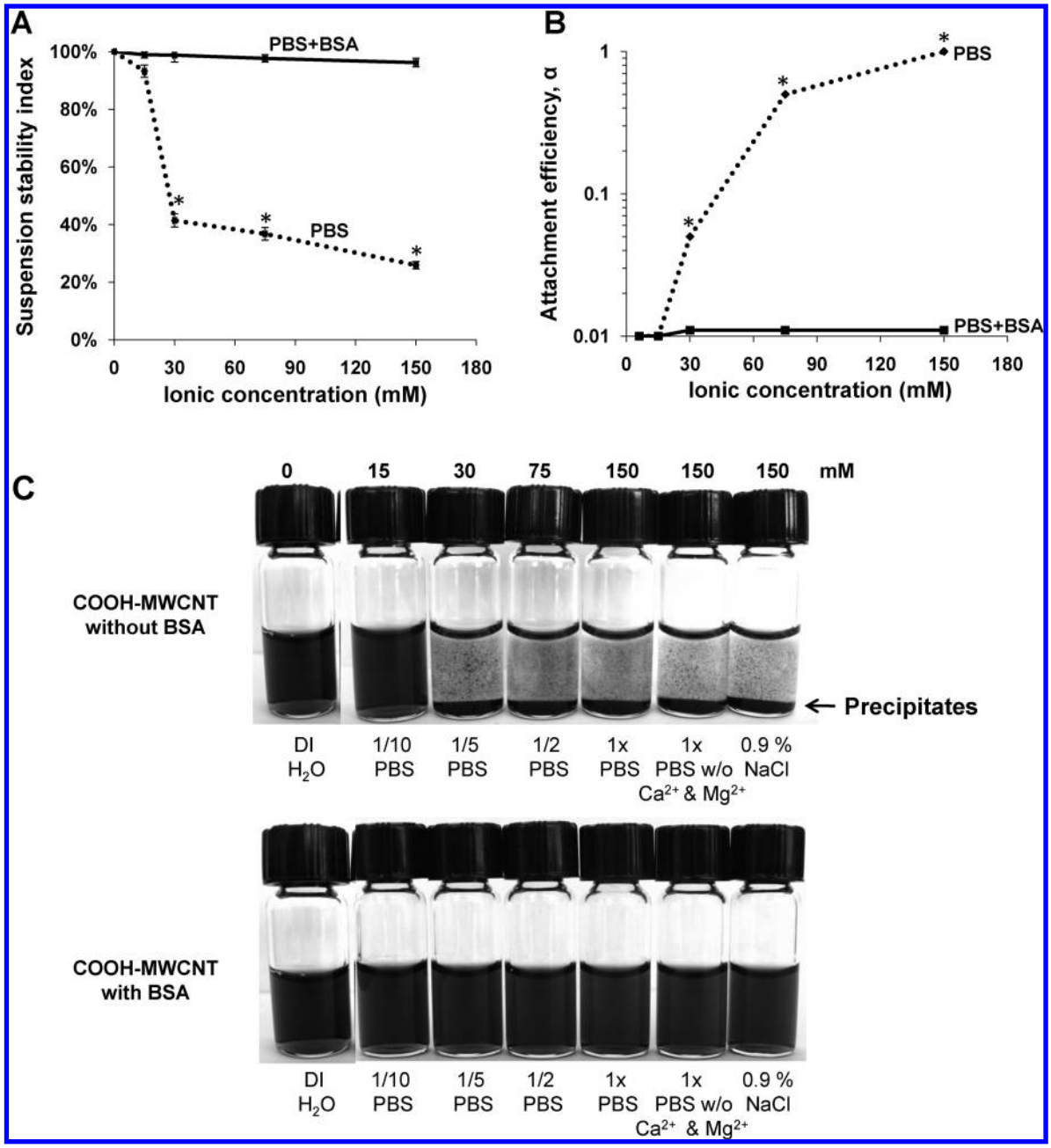

Figure 3. Solution ionic strength affects the suspension stability index and the attachment efficiency of MWCNTs in PBS and physiological media. (A) The suspension stability index of the COOH-MWCNTs at 50 μg/mL was expressed as the % of the initial absorbance (λ = 550 nm) for tubes incubated for 20 h after sonication in PBS concentrations of 0, 15, 30, 75, and 150 mM. The absorbance measurements were carried out by a UV−vis spectrometer (SpectroMax M5e, Molecular Devices Corp., Sunnyvale, CA) as described in Materials and Methods. (B) The attachment efficiency (α) of COOH-MWCNTs was calculated as a function of solution ionic strength. The attachment efficiency was calculated from the aggregation rate constant as described in Materials and Methods. (C) The effect of BSA (0.6 mg/mL) on COOH-MWCNT agglomeration as determined by visual inspection of precipitate formation in the presence of incremental PBS concentrations or 0.9% saline. The tubes were suspended by sonication as described in Materials and Methods in the absence or presence of 0.6 mg/mL BSA. The tubes were photographed 20 h after sonication.

mation and electrostatic screening of the wall charge, allowing the van der Waals forces to dominate (Supporting Information, Figure S4A). This leads to an increase of the attachment efficiency that can be quantitatively assessed by calculation of the α-factor for COOH-MWCNTs (Figure 3B). This calculation is made by using a laser to obtain DLS observations to feed into an equation that calculates an inverse stability ratio as demonstrated in Materials and Methods. Incremental PBS concentrations lead to a progressive increase in α (Figure 3B).

Because it is desirable to keep COOH-MWCNTs dispersed in ionic solutions, it is noteworthy that stable tube dispersions (>48 h) could be achieved by the addition of BSA to the PBS suspension (Figure 3A and 3C, lower panel). BSA is equally effective in DMEM, BEBM,

and BEGM (BEBM supplemented with essential growth factors) (Supporting Information, Figure S3). The improved dispersal of COOH-MWCNT is accompanied by decreased attachment efficiency in PBS (Figure 3B) and an increase in the tubes' suspension stability index (Figure 3A). While BSA binding to the carboxylated tubes may involve hydrophobic vacancies that are interspersed with the COOH groups, it is also possible that this protein could attach to the negatively charged tube surfaces *via* a Ca^{2+} bridge (Supporting Information, Figure S4B). This could provide steric and electrosteric hindrances that overcome the reduced electrostatic repulsion as a result of electrical double layer formation on the COOH-MWCNTs surface (Supporting Information, Figure S4A).

The Use of BSA and DPPC to Stabilize MWCNT Dispersion in Tissue Culture Media for Cellular Studies. Since BSA interacts with hydrophobic (AP, PD) as well as carboxylated MWCNTs to stabilize aqueous dispersions (Figure 3C and Supporting Information, Figure S3), we made use of the versatile properties of this protein to implement quantative and reproducible methods for MWCNT dispersal to perform tissue culture experiments. The effect of BSA was studied in parallel with DPPC use to compare the protein's effect to that of the phospholipid detergent.[21,23] To provide a quantitative assessment of the suspension stability index, we used UV−vis spectroscopy to assess time-dependent MWCNT sedimentation in the absence and presence of BSA and/or DPPC. The hierarchical order of the suspension stability index in BEGM was COOH-MWCNTs > PD-MWCNTs > AP-MWCNTs (Figure 4A). While DPPC coating did not improve the tendency to agglomerate, the addition of BSA significantly improved the stability index of PD-MWCNTs and AP-MWCNTs over a 20 h observation period (Figure 4A). Interestingly, while coadministration of DPPC significantly enhanced the ability of BSA to disperse the more hydrophobic AP-MWCNTs, this detergent had no added effects on PD- and COOH-MWCNT dispersal (Figure 4A). To determine whether the DPPC effect on AP-MWCNTs is additive to BSA, we also estimated the stability index using equimolar quantities of DPPC, BSA, and BSA+DPPC. This demonstrated that the combination of BSA and DPPC provided more stable dispersions than equimolar quantities of the individual dispersants (Figure 4B). BSA and DPPC were equally effective at dispersing tubes at lower (25 μg/mL) and higher (100 μg/mL) concentrations as demonstrated in Supporting Information, Figure S5. Thus, the combination of BSA and DPPC provides an additive effect for the more hydrophobic AP-MWCNTs. Whether this is due to random colocalization of the dispersants on the tube surface or a cooperative effect requires further study (Supporting Information, Figure S4C). Cooperative binding could involve interaction of the phospholipid fatty acid tails with the hydrophobic binding pockets that are being used for fatty acid transport. Thus, it is possible that cooperative binding on the tube surface could lead to a 3-way interaction between the tubes, BSA, and DPPC.

Similar results were obtained when adding BSA to the epithelial growth medium, DMEM, except that the protein alone provided efficient dispersal of all tube formulations in the absence of DPPC (Figure 5). The observation that DPPC was required as an additional dispersant in BEGM could be due to the addition of bovine pituitary growth factors to this culture medium to promote epithelial cell growth. The extract contains a number of biomolecules such as lipids, peptides, and proteins that could influence tube dispersal. Interestingly, the agglomeration rates for each of the tube formulations were slower in DMEM than in BEGM (compare Figure 4A with Figure 5). Because the former medium is often used with FBS supplementation to yield complete DMEM (cDMEM), we also assessed the stability index in cDMEM. Even though cDMEM contains BSA, it was not quite as effective for tube dispersal as BSA alone (Figure 5).

On the basis of the aforementioned findings, a mechanism for MWCNT deagglomeration can be proposed where tube sonication in the presence of dispersing agents can be used to obtain stable suspensions in tissue culture media. Sonication provides a local shear force that opens up spaces at the end of the tube bundles or stacks. Once formed, these spaces become occupied by protein or detergent-like dispersants that lead to smaller and more stable tube agglomerates.[30] BSA is an effective dispersant that provides steric as well as electrosteric hindrance. When dealing with tubes that have a highly hydrophobic surface (*e.g.*, the AP-MWCNT in this study), DPPC may provide additional stabilization of the BSA effect (Figure 4B). The implementation of quantitative methods for assessing tube stability in aqueous and ionic environments is a considerable improvement over more subjective techniques such as the use of light optical microscopy to visualize the agglomerate size. Nonetheless, the visual inspection confirms that BSA indeed leads to the forming of smaller tube stacks and that this effect is enhanced by DPPC when the more hydrophobic tubes are used in BEGM (data not shown). Although mathematically inaccurate for estimating the exact stack sizes, we could confirm that DLS is helpful for determining the relative hydrodynamic size of the tube agglomerates and can help to provide a semiquantitative estimation of BSA and/or DPPC dispersing effects in tissue culture media (Supporting Information, Figure S6A and Figure S6B).

The Dispersion State of MWCNTs Affects Bronchial Epithelial and Fibroblast Responses. Previous studies reported that intratracheal instillation of poorly dispersed SWCNTs (large agglomerates, ~1.5 μm diameter) results in tube deposition in the terminal bronchioles and proximal alveoli, where the tubes elicit granulomatous inflammation.[8,9] In contrast, well-dispersed SWCNTs

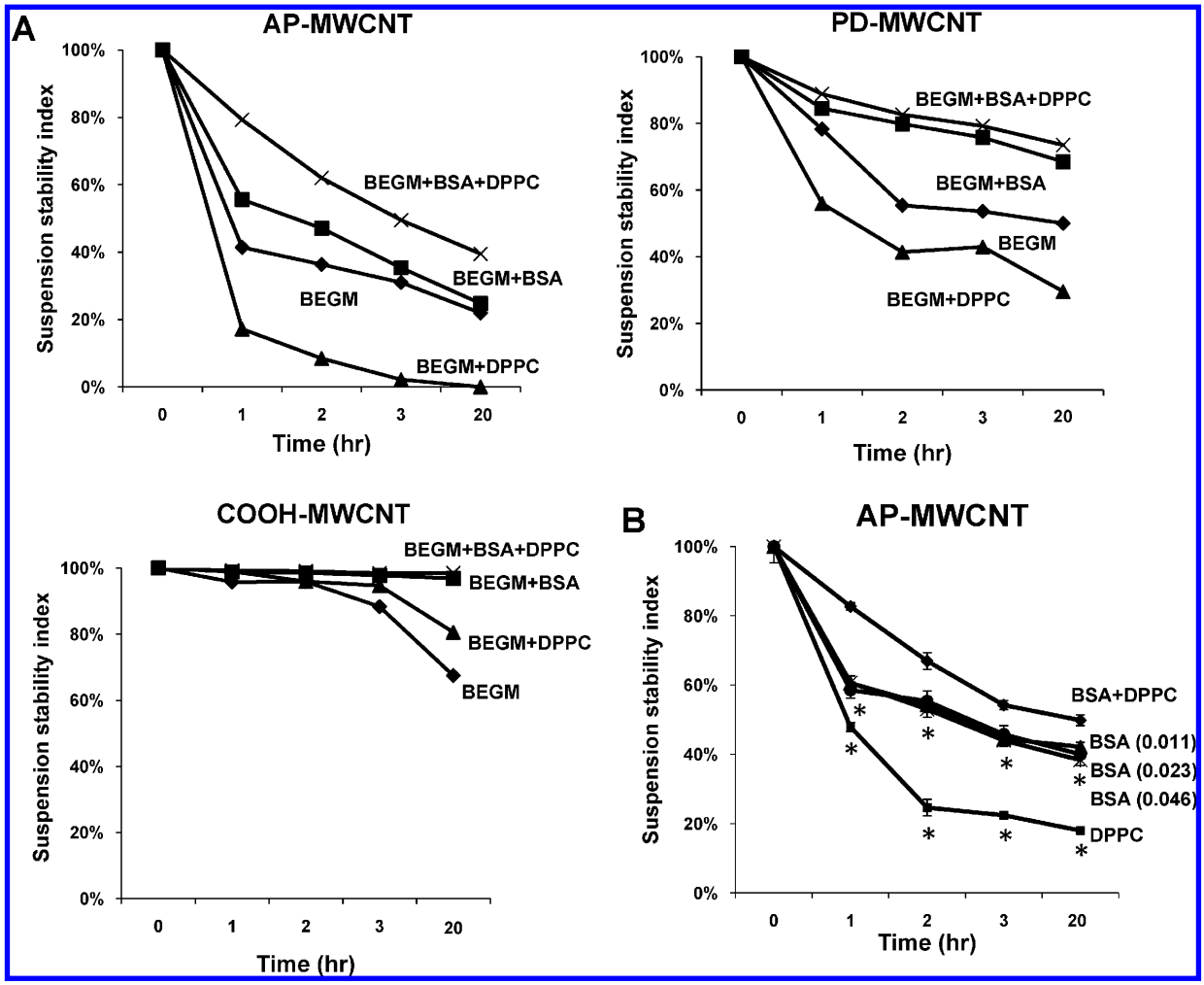

Figure 4. Stability of AP-MWCNT, PD-MWCNT, and COOH-MWCNT suspensions in BEGM in the absence or presence of dispersing agents [BSA (0.6 mg/mL) ± DPPC (0.01 mg/mL)]. (A) The suspension stability index of the MWCNT was determined as a function of time after suspension at 50 μg/mL in BEGM in the absence or presence of BSA, DPPC, or BSA+DPPC. The suspension stability index was calculated as the % of initial MWCNT absorbance ($t = 0$) at $\lambda = 550$ nm for time periods of 1, 2, 3, and 20 h. Absorbance was determined as described in Figure 3. The stability of the AP-MWCNT suspension in BEGM+BSA+DPPC differed significantly ($p < 0.05$) from the tubes being stabilized in BSA alone. (B) The effect of BSA plus DPPC on AP-MWCNT stabilization is additive compared to equimolar BSA or DPPC concentrations. The suspension stability index of the tubes sonicated in 0.023 mM total dispersants (BSA = 0.009 mM, DPPC = 0.014 mM) is compared to 0.023 or 0.046 mM BSA as well as 0.023 mM DPPC. The addition of BSA plus DPPC significantly ($p < 0.05$) enhanced AP-MWCNT stability compared to either BSA concentrations or an equimolar quantity of DPPC. BSA (0.011) = BSA at 0.011 mM; BSA (0.023) = BSA at 0.023 mM; BSA (0.046) = BSA at 0.046 mM in BEGM. Please notice that execution of the same experiment at different tube concentrations show BSA is capable of stabilizing the tubes in suspension over a wide dose range (see Supporting Information, Figure S5). The asterisks (*) denote $p < 0.05$ compared to the suspension stability index of AP-MWCNTs in BEGM+BSA+DPPC.

with a mean aggregate diameter of ~0.7 μm gain rapid access to the alveolar interstitial space where they induce a progressive fibrosis with minimal evidence of lung inflammation.[7,12] A key question becomes whether the dispersion state of MWCNTs affects cellular behavior, including biological responses that may be informative of pulmonary injury. To study the effects of tube dispersal states in a bronchial epithelial cell line, BEAS-2B, we first compared the tubes' influence on cell viability, LDH release and the production of TGF-β1, a fibroblast growth factor (Figure 6 and Supporting Information, Figure S7). While neither agglomerated nor dispersed tubes had any effect on cellular metabolic activity (MTS assay, Supporting Information, Figure S7A) or LDH release (Figure S7B), BEAS-2B cells did significantly increase TGF-β1 in production in response to well dispersed (BSA+DPPC) AP-MWCNTs and PD-MWCNTs (Figure 6). In contrast, agglomerated tubes that were not treated with a dispersant (ND) had no effect on TGF-β1 production (Figure 6). While small quantities of TGF-β1 were released from cells treated with COOH-MWCNTs, the addition of dispersants had no effect (Figure 6). To determine the relevance of TGF-β1 production on fibroblast growth potential, we also developed a proliferation assay using the human lung fibroblast cell line, CRL-1490. In this assay, the number of proliferating cells incorporating the fluorescent dye, EdU, is quantitatively expressed as a percentage of the total cell number (Hoechst nuclear staining) (Figure S8A). Because transfer of the BEAS-2B supernatants in-

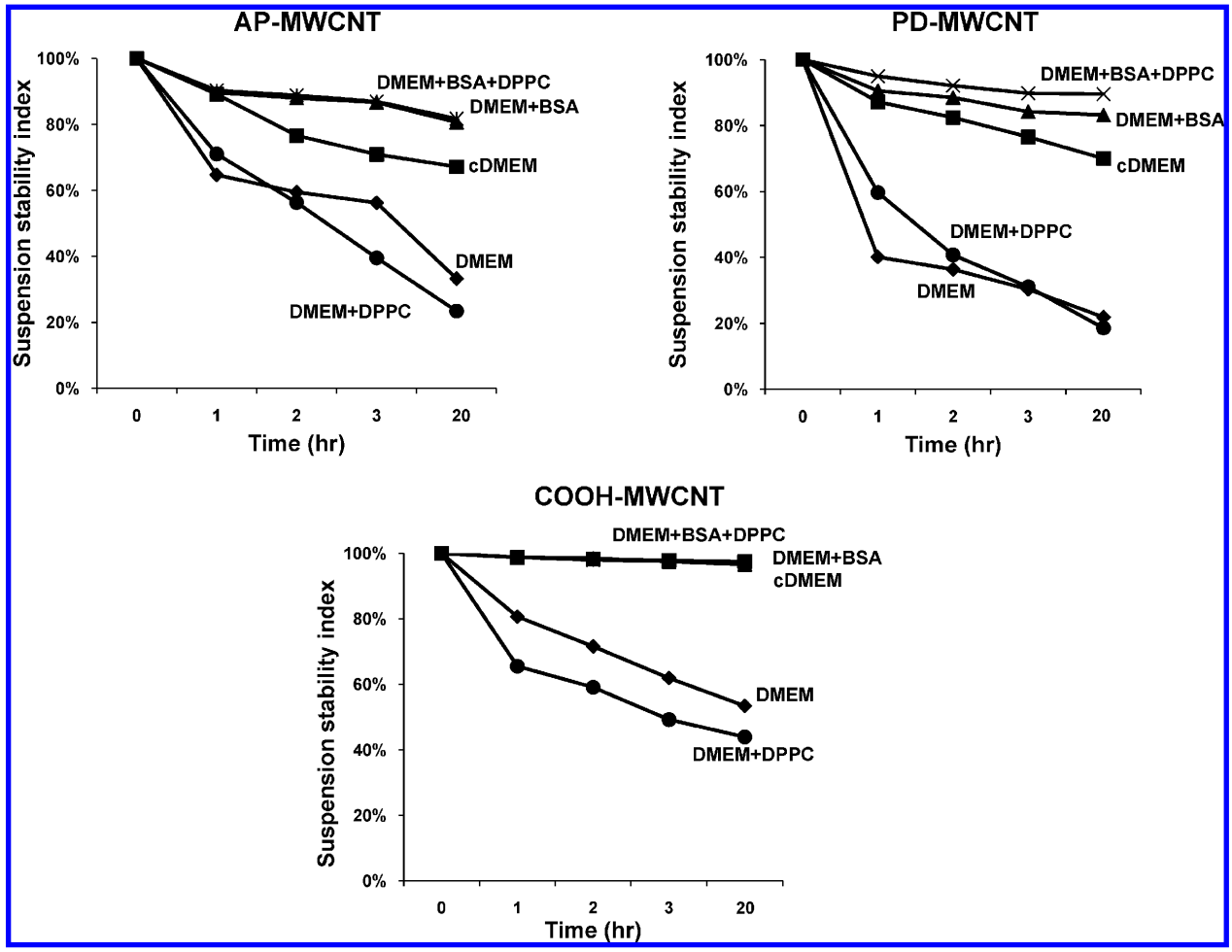

Figure 5. Assessment of the suspension stability index of AP-MWCNTs, PD-MWCNTs, and COOH-MWCNTs in DMEM, with or without the addition of dispersing agents [BSA (0.6 mg/mL), DPPC (0.01 mg/mL) and 10% FBS]. The suspension stability index of the MWCNTs in DMEM was determined as described in Figure 4A. The stability index is expressed as a percentage of the initial MWCNT absorbance (λ = 550 nm) as described in Figure 4.

terfered in CRL-1490 proliferation, we asked whether the exact amount of recombinant TGF-β1 (5−10 pg/mL) present in the BEAS-2B supernatant could induce CRL-1490 proliferation. Addition of 1.9−125 pg/mL TGF-β1 to the fibroblast culture medium increased the % EdU-positive cells in our fibroblast assay (Figure S8B). Moreover, direct addition of dispersed (D) versus non-dispersed (ND) MWCNT to the fibroblast culture me-

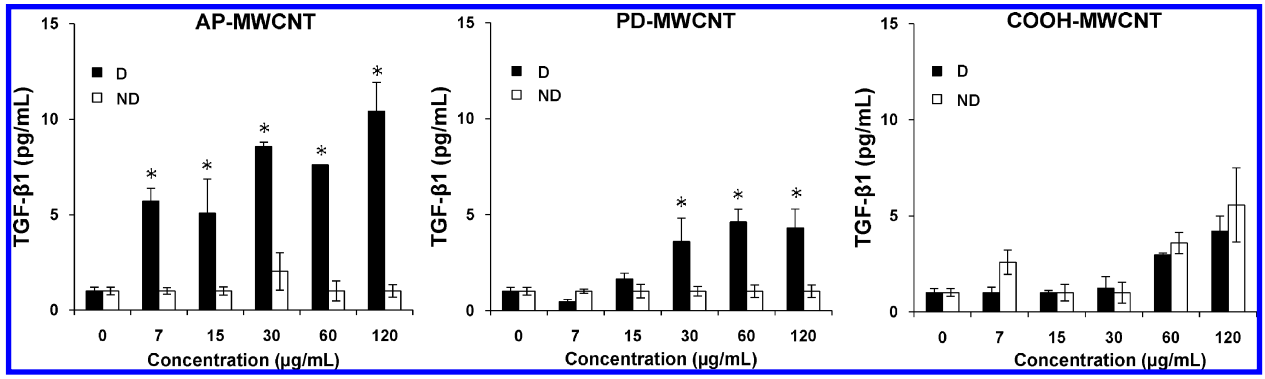

Figure 6. Comparison of the effect of dispersed (D) with nondispersed (ND) tubes on TGF-β1 release by BEAS-2B cells. Cells were treated with the indicated concentrations of the AP-, PD- and COOH-MWCNT that were either sonicated in the presence of BSA (0.6 mg/mL) + DPPC (0.01 mg/mL) for 24 h or vortexed in the absence of the dispersants (BSA and DPPC) or sonication. The supernatants were collected to measure the TGF-β1 levels by ELISA as described in Materials and Methods. Please notice that there was no TGF-β1 release in BEAS-2B cells in response to MWCNT exposures where tubes not dispersed in BSA were sonicated (data not shown). Thus, sonication by itself does not provide sufficient dispersion to influence biological response outcomes at the cellular level. The asterisks (*) denote $p < 0.05$, comparing nondispersed (ND) to dispersed (D) tubes.

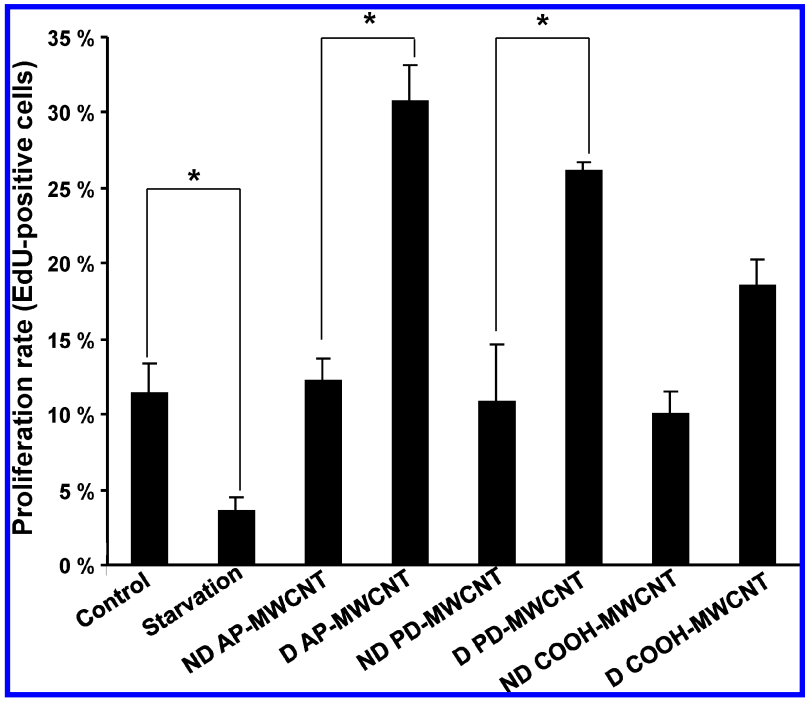

Figure 7. Fibroblast proliferation rate in response to MWCNT exposure. Fibroblast proliferation was assessed by an EdU proliferation assay. CRL-1490 cells (derived from pulmonary fibroblasts) were grown at a density of 5000 cells per well in 200 μL of EMEM supplemented with 10% FBS. Dispersed (D) and nondispersed (ND) MWCNTs were added to triplicate culture wells at a concentration of 5 μg/mL for 48 h. A starvation condition (containing 1% FBS) was included as a negative control. Cells were fixed and stained with the EdU and Hoechst dyes according to the manufacturer's instruction. Cells were viewed under an Axio Observer. D1 inverted microscope, (Carl Zeiss, Inc.). The number of proliferating cells incorporating the fluorescent dye EdU is quantitatively expressed as a percentage of the total cell population (Hoechst nuclear staining).

dium (Earl's Minimum Essential Medium, supplemented with 10% FBS) elicited fibroblast proliferation in the presence of dispersed AP and PD tubes, while ND tubes had no effect (Figure 7). In addition, dispersed COOH-MWCNT did not significantly increase fibroblast proliferation (Figure 7).

While it is clear that in the dispersed state there is a definitive increase in the cellular response with increased dose of AP- or PD-MWCNTs (Figure 6), it is important to make the point that dispersal could affect the bioavailable dose at the cellular level. While we do not understand as yet whether this translates into more tubes making contact with the cell membrane or more tubes being taken up into the cell, it is conceivable that both processes could be enhanced by better tube dispersal. In that case, improved tube dispersal could play a role in the local dosimetry that determines response outcome, either through cell membrane contact or intracellular uptake.

Hydrophobicity is a major factor that determines the dispersion state of AP-MWCNTs and PD-MWCNTs in water and cellular growth media. In contrast, the ionic strength of the solution is a major factor that influences the state of COOH-MWCNT agglomeration in buffered salt-containing media. In spite of these different forces contributing to the agglomeration of different tube versions, BSA is an effective dispersant that deagglomerates the tubes through a direct binding to the tube surfaces, using either hydrophobic or electrostatic binding interactions. BSA surface binding results in steric and electrosteric hindrances that are capable of stabilizing the MWCNTs in suspension. While BSA is quite effective for MWCNT dispersion in different media, DPPC provides additional stability for more hydrophobic MWCNTs in epithelial growth medium. Being able to perform quantitative assessment of the state of CNT dispersion or agglomeration in biological media is of importance for conducting mechanistic cellular studies that could inform us about adverse CNT effects in the lung. In this regard, we demonstrate that the dispersal state of AP- and PD-MWCNTs impacts TGF-β1 production and fibroblast proliferation, which could explain why better dispersed tubes are more potent than nondispersed tubes in inducing pulmonary fibrosis.[7] Our future studies will develop a predictive toxicological model based on these concepts. Being able to do high throughput comparison of CNTs in tissue culture cells can help to gather data in large CNT batches for subsequent use to perform *in vivo* studies.

In addition to its effect on the physicochemical state of MWCNT dispersion, it is important to consider that BSA coating of the tubes' surfaces could have an independent influence on biological outcomes from the perspective of either promoting cellular contact or uptake or preventing cellular contact or uptake due to steric hindrance effect. While these concepts have been more comprehensively studied with respect to engineered nanoparticles, less is known about this topic for CNTs, and several fundamental issues need to be addressed regarding contact of the CNTs with the cell membrane and possible intracellular uptake.[32,33] Kam *et al.* have suggested that SWCNTs are capable of traversing the cell membrane through endocytosis, whereas Pantarotto *et al.* have suggested that CNTs could be translocated into the cell through a process that involves insertion and diffusion through the lipid bilayer.[34,35] Moreover, Kam *et al.* have demonstrated that noncovalent conjugation of BSA or DNA to SWCNT surfaces leads to more avid tube uptake in HeLa and

HL60 cells. Although we did not look at cellular uptake in this study, it is important to consider the possibility that in the generation of fibrogenic responses BSA could contribute to promoting cellular contact with the MWCNTs. This would be equivalent to a scaffolding effect similar to the use of CNTs in tissue engineering to promote the growth and proliferation of stem cells. While clearly more work is required in this area, it is important to point out that the BSA concentration (0.6 mg/mL or 0.06%) we used in this study is very low and that from a pulmonary perspective this dose has been estimated to be 50 times less than undiluted alveolar lining fluid.[22] Moreover, Sager *et al*. and Porter *et al*. have shown that the experimental dose of BSA that we used does not alter the inflammatory potential of crystalline silica in rats or mice 1 day postexposure.[21,22] This suggests that BSA does not mask the bioactivity of these nanoparticles.

MATERIALS AND METHODS

Carbon Nanotubes and Chemicals. The MWCNT stock was purchased as a powder from Cheap Tubes, Inc. (Brattleboro, VT). The stock preparation is also referred to as as-prepared (AP) nanotubes. Bronchial epithelial growth medium (BEGM) was obtained from Lonza (Mapleton, IL), which is supplemented with a number of growth factors including bovine pituitary extract (BPE), insulin, hydrocortisone, hEGF, epinephrine, triiodothyronine, transferrin, gentamicin/amphotericin-B and retinoic acid. Dulbecco's modified eagle's medium (DMEM) with high glucose and phosphate buffered saline (PBS) were purchased from Invitrogen (Carlsbad, CA). Earl's Minimum Essential Medium (EMEM) was purchased from the American Type Culture Collection (ATCC, Manassas, VA, USA). Low-endotoxin bovine serum albumin (BSA) and fetal bovine serum (FBS) were from Gemini Bio-Products (West Sacramento, CA). Dipalmitoylphosphatidylcholine (DPPC) and *n*-octanol were purchased from Sigma-Aldrich (St. Louis, MO). All MWCNT stock solutions were prepared using pure deionized water (DI H_2O) with resistivity >18 MΩ-cm.

Physicochemical Characterization of MWCNT. The purification and functionalization of the MWCNT were accomplished as previously described.[36−38] This activity was carried out in a microwave accelerated reaction system CEM Mars (Matthews, NC) fitted with internal temperature and pressure controls. The 100 mL reaction chamber was lined with Teflon PFA with an operating range of 0−200 °C and 0−200 psi. The residual metals were removed *via* microwave induced reaction with 1 N HNO_3 followed by a reaction with saturated ethylenediamine tetra-acetate in CH_3COOH.[39] The purified MWCNT (PD-MWCNT) were added to the reaction chamber together with 40 mL of a mixture of 1:1 70% nitric acid and 97% sulfuric acid. With the microwave power set to 95% of the maximal possible 1600 W output, the reaction was carried out for 20 min at a temperature of 140 °C. The suspension was filtered through a 10 μm PTFE membrane, washed with deionized water (DI H_2O) to a neutral pH, and vacuum-dried at 70 °C. This sample derivative was designated COOH-MWCNT. A variety of different analytical techniques were used to characterize the MWCNTs, including energy dispersive X-ray spectroscopy (EDS, Oxford Instrument, Oxfordshire, UK) to identify the elemental composition of the MWCNTs. The Fourier transform infrared spectroscopy (FTIR) measurements were carried out in purified KBr pellets using a PerkinElmer Spectrum One instrument (Downers Grove, IL). Thermogravimetric analyses (TGA) were performed using a Pyris 1 TGA (Perkin-Elmer Inc., Covina, CA) from 30 to 900 °C under a flow of air at 10 mL/min and a heating rate of 10 °C per min. Scanning electron microscopy (SEM) using a LEO 1530 VP SEM equipped with an energy-dispersive X-ray analyzer was used to study the morphology of the samples. Zeta-potential measurements of the MWCNT suspensions were performed using a ZetaSizer Nano-ZS Instrument (Malvern Instruments, Worcestershire WR, UK). The relative hydrodynamic radius of MWCNTs suspended in H_2O was measured using high throughput dynamic light scattering (HT-DLS, Dynapro Plate Reader, Wyatt Technology, Santa Barbara, CA).

Preparation of MWCNT Suspension in Media. AP-, PD-, and COOH-MWCNTs were provided as dry powders. The samples were weighed on an analytical balance in the fume hood and suspended in DI H_2O at a concentration of 5 mg/mL in 4 mL glass vials. These suspensions were sonicated for 15 min in a water sonicator bath (Branson, Danbury, CT, model 2510, 100 W output power; 42 kHz frequency) and used as the stock solution for further dispersion in cell culture media. A water bath rather than a sonication probe was used to deliver a cavitation force suitable for deagglomeration but not so high as to prevent protein attachment or tube damage.[40−42] An appropriate amount of each stock solution was added to achieve the desired final concentration. The diluted tube suspensions were vortexed for 15 s (fixed-speed vortex, 02-215-360, Fisher Scientific, Pittsburgh, PA), sonicated for 15 min, and then vortexed for another 15 s vortex to obtain tube suspensions of 50 μg/mL (unless otherwise specified). Where dispersing agents were used, these were added to the culture media before the addition of the tubes. The final concentrations of BSA and DPPC were 0.6 mg/mL and 0.01 mg/mL, respectively, unless otherwise stated.

Assessment of the Hydrophobicity Index of MWCNT in Physiological Media. Partitioning of MWCNTs in an *n*-octanol/aqueous interface was used to calculate a hydrophobicity index.[43,44] After the MWCNTs were suspended in the various aqueous media at a range (25−100 μg/mL) of concentrations, the absorbance (*A*) of the tubes was measured at 550 nm by UV−vis spectrometry (SpectroMax M5e, Molecular Devices Corp., Sunnyvale, CA) based on previous work.[45] This value was designated A_0. An identical volume of *n*-octanol was added to the aqueous tube suspension, and the vials were vortexed for 15 s and then incubated at room temperature for 30 min. At this point the *A* value of the aqueous layer was remeasured (A_1), and hydrophobicity index (%) was calculated as follows:

$$\text{hydrophobicity index} = \left(\frac{A_0 - A_1}{A_0}\right) \times 100\%$$

Characterization of MWCNT Suspension Stability Index. A kinetic analysis of suspension stability was performed by monitoring the aqueous solution absorbance at 550 nm for different lengths of time, using UV−vis spectrometry (SpectroMax M5e, Molecular Devices Corp., Sunnyvale, CA). Typically, 1 mL of the MWCNT suspension at 25−100 μg/mL was prepared with or without dispersing agents and absorbance readings were taken at 1 h time intervals for 20 h.

Attachment Efficiency of COOH-MWCNT. A 90° light scattering unit (Malvern Instruments Zetasizer Nano ZS90, Worcestershire WR, UK) equipped with a 4 mW He−Ne laser with a frequency output of 632.8 nm was used to perform the CNT aggregation experiments. Agglomeration data were collected on 1 mg/mL dispersions of COOH-MWCNT in PBS and PBS + 0.6 mg/mL BSA. The PBS concentrations ranged from 6 to 150 mM. The dynamic light scattering measurements were collected at 25 °C. The incident laser beam and the autocorrelation function were allowed to accumulate for >10 s after a 120 min temperature equilibration. The measurements were performed for a period of time ranging from 150 s to 3 h. The initial rate of change in the hydrodynamic radius (R_h), $(dR_h/dt)_{t\to 0}$ is proportional to kn_o where *k* is the initial aggregation rate constant and n_o is the initial concentration of the MWCNT.[46] The inverse stability ratio α or attachment efficiency was obtained from the following equation:

$$\alpha = \frac{\left(\frac{dR_h}{dt}\right)_{t\to 0}}{\left(\frac{dR_h}{dt}\right)_{(f)t\to 0}}$$

where $(dR_h/dt)_{(f)t\to 0}$ represents the fast aggregation regime.[18,47,48]

BEAS-2B Cellular Culture and Co-incubation with MWCNTs. BEAS-2B cells were purchased from ATCC (Manassas, VA) and cultured in 5% CO_2 at 37 °C in BEGM in collagen-coated 75 cm^2 flasks. For exposure to MWCNTs, aliquots of 1×10^4 cells were cultured in 0.2 mL of medium in 96-well plates (Costar, Corning, NY) at 37 °C for the indicated time periods. All the MWCNT solutions were freshly prepared. While nondispersed (ND) MWCNTs were vortexed for 15 s but not sonicated in BEGM that also contained no dispersants (BSA, DPPC, or FBS), better dispersed (D) MWCNTs were prepared by sonication in BEGM containing BSA (at 0.6 mg/mL), DPPC (at 0.01 mg/mL) or a combination of both dispersants before being added to the tissue culture dishes.

ELISA for TGF-β1 Quantification. The TGF-β1 concentration in the BEAS-2B culture medium was determined by an E_{max} ImmunoAssay System (Promega, Madison, WI) according to the manufacturer's instructions. A 96-well plate was coated with monoclonal anti-TGF-β1, and the captured growth factor was detected by polyclonal anti-TGF-β1 conjugated to horseradish peroxidase. Absorbance was measured at 450 nm using a plate reader (SpectroMax M5e, Molecular Devices Corp., Sunnyvale, CA). Results were expressed as pg/mL.

Assessment of Fibroblast Proliferation using the EdU-Based Proliferation Assay. The human lung fibroblast cell line, CRL1490, was obtained from the American Type Culture Collection (Manassas, VA). The cells were cultured in EMEM supplemented with 10% FBS, 100 U/mL penicillin and 100 μg/mL streptomycin. Cultures were maintained in a 5% CO_2 humidified atmosphere at 37 °C. MWCNTs were added to the culture medium to a final concentration of 5 μg/mL, following which the suspensions were either (i) vortexed for 15 s, sonicated for 15 min, and vortexed again for 15 s to obtain dispersed (D) tubes or (ii) vortexed without sonication to obtain the nondispersed (ND) tube suspension. After exposure to the dispersed (D) and nondispersed (ND) MWCNTs for 48 h, CRL-1490 cells were fixed and stained with the EdU and Hoechst dyes according to manufacturer's instructions included in the Click-iT EdU cell proliferation kit (Invitrogen, Carlsbad, CA). Growth proliferation was assessed by calculating the percentage of cells in the culture that incorporates the fluorescent EdU into newly synthesized DNA. Please notice that because the EMEM is similar to the DMEM composition, there were no differences in the hydrophobicity index, suspension stability index, rate of agglomeration, and dynamic light scattering results in the former medium (not shown).

Acknowledgment. This work was funded by the National Science Foundation and the Environmental Protection Agency under Cooperative Agreement Number DBI-0830117. Any opinions, findings, and conclusions or recommendations expressed in this material are those of the author(s) and do not necessarily reflect the views of the National Science Foundation or the Environmental Protection Agency, or the National Institute for Occupational Safety and Health. This work has not been subjected to EPA review and no official endorsement should be inferred. Support for this work was also by the U.S. Public Health Service Grants, RC2 ES018766, RO1 CA133697, RO1 ES016746, and U19 ES019528 (UCLA Center for Nanobiology and Predictive Toxicology).

Supporting Information Available: Additional figures, results, and method descriptions as described in the text. This material is available free of charge *via* the Internet at http://pubs.acs.org.

REFERENCES AND NOTES

1. Iijima, S. Helical Microtubules of Graphitic Carbon. *Nature* **1991**, *354*, 56–58.
2. Lin, Y.; Taylor, S.; Li, H. P.; Fernando, K. A. S.; Qu, L. W.; Wang, W.; Gu, L. R.; Zhou, B.; Sun, Y. P. Advances Toward Bioapplications of Carbon Nanotubes. *J. Mater. Chem.* **2004**, *14*, 527–541.
3. Baughman, R. H.; Zakhidov, A. A.; de Heer, W. A. Carbon Nanotubes—The Route toward Applications. *Science* **2002**, *297*, 787–792.
4. Nel, A.; Xia, T.; Madler, L.; Li, N. Toxic Potential of Materials at the Nanolevel. *Science* **2006**, *311*, 622–627.
5. Muller, J.; Delos, M.; Panin, N.; Rabolli, V.; Huaux, F.; Lison, D. Absence of Carcinogenic Response to Multiwall Carbon Nanotubes in a 2-Year Bioassay in the Peritoneal Cavity of the Rat. *Toxicol. Sci.* **2009**, *110*, 442–448.
6. Muller, J.; Huaux, F.; Moreau, N.; Misson, P.; Heilier, J. F.; Delos, M.; Arras, M.; Fonseca, A.; Nagy, J. B.; Lison, D. Respiratory Toxicity of Multiwall Carbon Nanotubes. *Toxicol. Appl. Pharmacol.* **2005**, *207*, 221–231.
7. Shvedova, A. A.; Kisin, E. R.; Mercer, R.; Murray, A. R.; Johnson, V. J.; Potapovich, A. I.; Tyurina, Y. Y.; Gorelik, O.; Arepalli, S.; Schwegler-Berry, D. Unusual Inflammatory and Fibrogenic Pulmonary Responses to Single-Walled Carbon Nanotubes in Mice. *Am. J. Physiol.-Lung Cell. Mol. Physiol.* **2005**, *289*, L698–L708.
8. Warheit, D. B.; Laurence, B. R.; Reed, K. L.; Roach, D. H.; Reynolds, G. A. M.; Webb, T. R. Comparative Pulmonary Toxicity Assessment of Single-Wall Carbon Nanotubes in Rats. *Toxicol. Sci.* **2004**, *77*, 117–125.
9. Lam, C. W.; James, J. T.; McCluskey, R.; Hunter, R. L. Pulmonary Toxicity of Single-Wall Carbon Nanotubes in Mice 7 and 90 Days after Intratracheal Instillation. *Toxicol. Sci.* **2004**, *77*, 126–134.
10. Chou, C. C.; Hsiao, H. Y.; Hong, Q. S.; Chen, C. H.; Peng, Y. W.; Chen, H. W.; Yang, P. C. Single-Walled Carbon Nanotubes Can Induce Pulmonary Injury in Mouse Model. *Nano Lett.* **2008**, *8*, 437–445.
11. Meng, H.; Xia, T.; George, S.; Nel, A. E. A Predictive Toxicological Paradigm for the Safety Assessment of Nanomaterials. *ACS Nano* **2009**, *3*, 1620–1627.
12. Mercer, R. R.; Scabilloni, J.; Wang, L.; Kisin, E.; Murray, A. R.; Schwegler-Berry, D.; Shvedova, A. A.; Castranova, V. Alteration of Deposition Pattern and Pulmonary Response as a Result of Improved Dispersion of Aspirated Single-Walled Carbon Nanotubes in a Mouse Model. *Am. J. Physiol., Lung Cell. Mol. Physiol.* **2008**, *294*, L87–L97.
13. Girifalco, L. A.; Hodak, M.; Lee, R. S. Carbon Nanotubes, Buckyballs, Ropes, and a Universal Graphitic Potential. *Phys. Rev. B* **2000**, *62*, 13104–13110.
14. Liu, J.; Casavant, M. J.; Cox, M.; Walters, D. A.; Boul, P.; Lu, W.; Rimberg, A. J.; Smith, K. A.; Colbert, D. T.; Smalley, R. E. Controlled Deposition of Individual Single-Walled Carbon Nanotubes on Chemically Functionalized Templates. *Chem. Phys. Lett.* **1999**, *303*, 125–129.
15. Ausman, K. D.; Piner, R.; Lourie, O.; Ruoff, R. S.; Korobov, M. Organic Solvent Dispersions of Single-Walled Carbon Nanotubes: Toward Solutions of Pristine Nanotubes. *J. Phys. Chem. B* **2000**, *104*, 8911–8915.
16. Kang, S.; Mauter, M. S.; Elimelech, M. Microbial Cytotoxicity of Carbon-Based Nanomaterials: Implications for River Water and Wastewater Effluent. *Environ. Sci. Technol.* **2009**, *43*, 2648–2653.
17. Hyung, H.; Kim, J. H. Natural Organic Matter (NOM) Adsorption to Multiwalled Carbon Nanotubes: Effect of NOM Characteristics and Water Quality Parameters. *Environ. Sci. Technol.* **2008**, *42*, 4416–4421.
18. Saleh, N. B.; Pfefferle, L. D.; Elimelech, M. Aggregation Kinetics of Multiwalled Carbon Nanotubes in Aquatic Systems: Measurements and Environmental Implications. *Environ. Sci. Technol.* **2008**, *42*, 7963–7969.
19. Shvedova, A. A.; Castranova, V.; Kisin, E. R.; Schwegler-Berry, D.; Murray, A. R.; Gandelsman, V. Z.; Maynard, A.; Baron, P. Exposure to Carbon Nanotube Material: Assessment of Nanotube Cytotoxicity Using Human Keratinocyte Cells. *J. Toxicol. Environ. Health, Part A.* **2003**, *66*, 1909–1926.
20. Jia, G.; Wang, H. F.; Yan, L.; Wang, X.; Pei, R. J.; Yan, T.; Zhao,

Y. L.; Guo, X. B. Cytotoxicity of Carbon Nanomaterials: Single-Wall Nanotube, Multiwall Nanotube, and Fullerene. *Environ. Sci. Technol.* **2005**, *39*, 1378–1383.
21. Sager, T. M.; Porter, D. W.; Robinson, V. A.; Lindsley, W. G.; Schwegler-Berry, D. E.; Castranova, V. Improved Method to Disperse Nanoparticles for *in Vitro* and *in Vivo* Investigation of Toxicity. *Nanotoxicology* **2007**, *1*, 118–129.
22. Porter, D.; Sriram, K.; Wolfarth, M.; Jefferson, A.; Schwegler-Berry, D.; Andrew, M.; Castranova, V. A Biocompatible Medium for Nanoparticle Dispersion. *Nanotoxicology* **2008**, *2*, 144–154.
23. Elgrabli, D.; Abella-Gallart, S.; Aguerre-Chariol, O.; Robidel, F.; Rogerieux, F.; Boczkowski, J.; Lacroix, G. Effect of BSA on Carbon Nanotube Dispersion for *in Vivo* and *in Vitro* Studies. *Nanotoxicology* **2007**, *1*, 266–278.
24. Vaisman, L.; Wagner, H. D.; Marom, G. The Role of Surfactants in Dispersion of Carbon Nanotubes. *Adv. Colloid Interface Sci.* **2006**, *128*, 37–46.
25. Rector, D. R.; Bunker, B. C. Effect of Colloidal Aggregation on the Sedimentation and Rheological Properties of Tank Waste. Report No. PNL-10761; Pacific Norwest Laboratories: 1995; pp 2.42.5, DOI: 10.2172/113874.
26. Xia, T.; Kovochich, M.; Liong, M.; Zink, J. I.; Nel, A. E. Cationic Polystyrene Nanosphere Toxicity Depends on Cell-Specific Endocytic and Mitochondrial Injury Pathways. *ACS Nano* **2008**, *2*, 85–96.
27. Xia, T.; Kovochich, M.; Liong, M.; Madler, L.; Gilbert, B.; Shi, H. B.; Yeh, J. I.; Zink, J. I.; Nel, A. E. Comparison of the Mechanism of Toxicity of Zinc Oxide and Cerium Oxide Nanoparticles Based on Dissolution and Oxidative Stress Properties. *ACS Nano* **2008**, *2*, 2121–2134.
28. Ji, Z.; Jin, X.; George, S.; Xia, T.; Meng, H.; Wang, X.; Suarez, E.; Zhang, H.; Hoek, E. M.; Godwin, H.; *et al*. Dispersion and Stability Optimization of TiO(2) Nanoparticles in Cell Culture Media. *Environ. Sci. Technol.* **2010**, *44*, 7309–7314.
29. Chen, R. J.; Bangsaruntip, S.; Drouvalakis, K. A.; Kam, N. W. S.; Shim, M.; Li, Y. M.; Kim, W.; Utz, P. J.; Dai, H. J. Noncovalent Functionalization of Carbon Nanotubes for Highly Specific Electronic Biosensors. *Proc. Natl. Acad. Sci. U.S.A.* **2003**, *100*, 4984–4989.
30. Strano, M. S.; Moore, V. C.; Miller, M. K.; Allen, M. J.; Haroz, E. H.; Kittrell, C.; Hauge, R. H.; Smalley, R. E. The Role of Surfactant Adsorption During Ultrasonication in the Dispersion of Single-Walled Carbon Nanotubes. *J. Nanosci. Nanotechnol.* **2003**, *3*, 81–86.
31. Wang, L. Y.; Mercer, R. R.; Rojanasakul, Y.; Qiu, A. J.; Lu, Y. J.; Scabilloni, J. F.; Wu, N. Q.; Castranova, V. Direct Fibrogenic Effects of Dispersed Single-Walled Carbon Nanotubes on Human Lung Fibroblasts. *J. Toxicol. Environ. Health, Part A.* **2010**, *73*, 410–422.
32. Wilhelm, C.; Billotey, C.; Roger, J.; Pons, J. N.; Bacri, J. C.; Gazeau, F. Intracellular Uptake of Anionic Superparamagnetic Nanoparticles as a Function of Their Surface Coating. *Biomaterials* **2003**, *24*, 1001–1011.
33. Kratz, F. Albumin as a Drug Carrier: Design of Prodrugs, Drug Conjugates, and Nanoparticles. *J. Contr. Release* **2008**, *132*, 171–183.
34. Kam, N. W. S.; Liu, Z. A.; Dai, H. J. Carbon Nanotubes as Intracellular Transporters for Proteins and DNA: An Investigation of the Uptake Mechanism and Pathway. *Angew. Chem., Int. Ed.* **2006**, *45*, 577–581.
35. Pantarotto, D.; Briand, J. P.; Prato, M.; Bianco, A. Translocation of Bioactive Peptides across Cell Membranes by Carbon Nanotubes. *Chem. Commun.* **2004**, *1*, 16–17.
36. Wang, Y. B.; Iqbal, Z.; Mitra, S. Microwave-Induced Rapid Chemical Functionalization of Single-Walled Carbon Nanotubes. *Carbon* **2005**, *43*, 1015–1020.
37. Wang, Y. B.; Iqbal, Z.; Mitra, S. Rapidly Functionalized, Water-Dispersed Carbon Nanotubes at High Concentration. *J. Am. Chem. Soc.* **2006**, *128*, 95–99.
38. Wang, Y.; Iqbal, Z.; Mitra, S. Rapid, Low Temperature Microwave Synthesis of Novel Carbon Nanotube−Silicon Carbide Composite. *Carbon* **2006**, *44*, 2804–2808.
39. Chen, Y. H.; Mitra, S. Fast Microwave-Assisted Purification, Functionalization, and Dispersion of Multiwalled Carbon Nanotubes. *J. Nanosci. Nanotechnol.* **2008**, *8*, 5770–5775.
40. Thess, A.; Lee, R.; Nikolaev, P.; Dai, H. J.; Petit, P.; Robert, J.; Xu, C. H.; Lee, Y. H.; Kim, S. G.; Rinzler, A. G. Crystalline Ropes of Metallic Carbon Nanotubes. *Science* **1996**, *273*, 483–487.
41. Oberdorster, G.; Maynard, A.; Donaldson, K.; Castranova, V.; Fitzpatrick, J.; Ausman, K.; Carter, J.; Karn, B.; Kreyling, W.; Lai, D.; *et al*. Principles for Characterizing the Potential Human Health Effects from Exposure to Nanomaterials: Elements of a Screening Strategy. *Part. Fibre Toxicol.* **2005**, *2*, 8.
42. Deguchi, S.; Yamazaki, T.; Mukai, S.; Usami, R.; Horikoshi, K. Stabilization of C-60 Nanoparticles by Protein Adsorption and Its Implications for Toxicity Studies. *Chem. Res. Toxicol.* **2007**, *20*, 854–858.
43. Chen, W.; Duan, L.; Zhu, D. Adsorption of Polar and Nonpolar Organic Chemicals to Carbon Nanotubes. *Environ. Sci. Technol.* **2007**, *41*, 8295–8300.
44. George, S.; Kishen, A. Effect of Tissue Fluids on Hydrophobicity and Adherence of Enterococcus Faecalis to Dentin. *J. Endod.* **2007**, *33*, 1421–1425.
45. Worsley, K. A.; Kalinina, I.; Bekyarova, E.; Haddon, R. C. Functionalization and Dissolution of Nitric Acid Treated Single-Walled Carbon Nanotubes. *J. Am. Chem. Soc.* **2009**, *131*, 18153–18158.
46. Schudel, M.; Behrens, S. H.; Holthoff, H.; Kretzschmar, R.; Borkovec, M. Absolute Aggregation Rate Constants of Hematite Particles in Aqueous Suspensions: A Comparison of Two Different Surface Morphologies. *J. Colloid Interface Sci.* **1997**, *196*, 241–253.
47. Chen, K. L.; Elimelech, M. Influence of Humic Acid on the Aggregation Kinetics of Fullerene (C-60) Nanoparticles in Monovalent and Divalent Electrolyte Solutions. *J. Colloid Interface Sci.* **2007**, *309*, 126–134.
48. Chen, K. L.; Mylon, S. E.; Elimelech, M. Aggregation Kinetics of Alginate-Coated Hematite Nanoparticles in Monovalent and Divalent Electrolytes. *Environ. Sci. Technol.* **2006**, *40*, 1516–1523.